



1 **Improving the representation of high-latitude vegetation in**
2 **Dynamic Global Vegetation Models**

3
4 Peter Horvath^{1,4}, Hui Tang^{1,2,4}, Rune Halvorsen¹, Frode Stordal^{2,4}, Lena Merete Tallaksen^{4,5},
5 Terje Koren Berntsen^{2,4}, Anders Bryn^{1,3,4}

6
7 ¹ Geo-Ecology Research Group, Natural History Museum, University of Oslo, P.O. Box 1172, Blindern NO-0318
8 Oslo, Norway

9 ² Section of Meteorology and Oceanography, Department of Geosciences, University of Oslo, Norway

10 ³ Division of Survey and Statistics, Norwegian Institute of Bioeconomy Research, P.O. Box 115, NO-1431 Ås,
11 Norway

12 ⁴ LATICE Research Group, Department of Geosciences, University of Oslo, Norway

13 ⁵ Section of Physical geography and Hydrology, Department of Geosciences, University of Oslo, Norway

14

15 Correspondence to: Horvath, P. (peter.horvath@nhm.uio.no)

16 **Keywords:** Area frame survey, Community Land Model, CLM4.5BGCDV, Distribution model, Earth System
17 Model, Plant functional types, Remote sensing, Vegetation types,

18



19 **Abstract.** Vegetation is an important component in global ecosystems, affecting the physical, hydrological and
20 biogeochemical properties of the land surface. Accordingly, the way vegetation is parameterised strongly
21 influences predictions of future climate by Earth system models. To capture future spatial and temporal changes
22 in vegetation cover and its feedbacks to the climate system, dynamic global vegetation models (DGVM) are
23 included as important components of land surface models. Variation in the predicted vegetation cover from
24 DGVMs therefore has large impacts on modelled radiative and non-radiative properties, especially over high-
25 latitude regions. DGVMs are mostly evaluated by remotely sensed products, but rarely by other vegetation
26 products or by in-situ field observations. In this study, we evaluate the performance of three methods for spatial
27 representation of vegetation cover with respect to prediction of plant functional type (PFT) profiles – one based
28 upon distribution models (DM), one that uses a remote sensing (RS) dataset and a DGVM (CLM4.5BGCDV).
29 PFT profiles obtained from an independently collected vegetation data set from Norway were used for the
30 evaluation. We found that RS-based PFT profiles matched the reference dataset best, closely followed by DM,
31 whereas predictions from DGVM often deviated strongly from the reference. DGVM predictions overestimated
32 the area covered by boreal needleleaf evergreen trees and bare ground at the expense of boreal broadleaf deciduous
33 trees and shrubs. Based on environmental predictors identified by DM as important, we suggest implementation
34 of three novel PFT-specific thresholds for establishment in the DGVM. We performed a series of sensitivity
35 experiments to demonstrate that these thresholds improve the performance of the DGVM. The results highlight
36 the potential of using PFT-specific thresholds obtained by DM in development and benchmarking of DGVMs for
37 broader regions. Also, we emphasize the potential of establishing DM as a reliable method for providing PFT
38 distributions for evaluation of DGVMs alongside RS.



39 1 Introduction

40 Vegetation plays an important role in the climate system, as changes in the vegetation cover alter the
41 biogeophysical and biogeochemical properties of the land surface (Davin and de Noblet-Ducoudré, 2010;
42 Duveiller et al., 2018). Therefore an accurate descriptions of the vegetation distribution hold a key role in Earth
43 system models (ESM) (Bonan, 2016; Poulter et al., 2015). Historical and present vegetation distributions are
44 implemented in ESMs by means of datasets prepared from satellite observations (Lawrence and Chase, 2007; Li
45 et al., 2018; Lawrence et al., 2011). However, in order to predict the future temporal and spatial changes in natural
46 vegetation cover and subsequently the processes, dynamics and feedbacks to the climate system, dynamic global
47 vegetation models (DGVMs) are needed.

48 DGVMs have been implemented as components of ESMs (Bonan et al., 2003) to represent long-term vegetation
49 changes by a set of parameterizations describing general physiological principles, including ecological
50 disturbances, successions (Seo and Kim, 2019) and species interactions (Scheiter et al., 2013). DGVMs represent
51 the heterogeneity of land surface processes and interactions with other components of the Earth system by
52 characterising land areas by their composition of type units defined by plant functional types (PFTs) (Bonan et al.,
53 2003; Oleson et al., 2013). PFTs are groupings of plant species with similar eco-physiological properties – which
54 express differences in growth form (woody vs herbaceous), leaf longevity (deciduous vs evergreen) and
55 photosynthetic pathway (C3 and C4) (Wullschleger et al., 2014). Even though the DGVMs are being constantly
56 developed and improved to incorporate more complex plant processes (Fisher et al., 2010), there are still
57 fundamental challenges for DGVMs to correctly simulate the extents of the PFTs that characterise boreal and
58 Arctic ecoregions (Gotangco Castillo et al., 2012). For instance, the thematic resolution of high-latitude PFTs is
59 still limited (Wullschleger et al., 2014), important interactions between vegetation and fire in high latitudes are
60 still missing (Seo and Kim, 2019), and forest carbon storage in the high latitude is still underestimated by most
61 DGVMs (Song et al., 2013). The large uncertainties in simulating high-latitude PFT distributions may also lead to
62 discrepancies between modelled and observed energy fluxes and hydrology (Hartley et al., 2017) or carbon cycles
63 (Sitch et al., 2008). Accordingly, systematic evaluation of PFT distributions modelled by DGVMs is required to
64 improve the DGVMs and, subsequently, to reduce uncertainties in estimates of climate sensitivity and in
65 predictions by ESMs.

66 Remote sensing (RS) is often used for evaluation, benchmarking and improvement of parameters in of DGVMs
67 (Zhu et al., 2018). RS products are commonly used to describe vegetation cover using vegetation classes derived
68 from multispectral images based on vegetation indices such as the normalized difference vegetation index (NDVI)
69 (Xie et al., 2008; Franklin and Wulder, 2002). For evaluation, RS products are translated into distributions of the
70 PFT classes used in the DGVMs (Lawrence and Chase, 2007; Poulter et al., 2011). However, inconsistencies
71 between various available RS-based land cover or vegetation products have been reported (Myers-Smith et al.,
72 2011) and benchmarking DGVMs only to these RS-based products may therefore lead to different conclusions in
73 ESMs (Poulter et al., 2015).

74 Among the less explored methods to generate wall-to-wall vegetation cover predictions is distribution modelling.
75 Distribution models (DMs) are most often used to predict the distribution of a target, by establishment of statistical
76 relationship between the target (response) and the environment (predictors) (e.g. Halvorsen, 2012). The most
77 common use of DM in ecology is for prediction of species distributions (Henderson et al., 2014), but DM methods
78 have proved valuable also for prediction of targets at higher levels of bio-, geo- or eco-diversity (i.e. vegetation



79 types and land-cover types) (Ullerud et al., 2016; Horvath et al., 2019; Simensen et al., accepted). DM methods
80 are inherently static, in contrast to the dynamic DGVMs (Snell et al., 2014). Nevertheless, they may be a useful
81 corrective to DGVMs by providing insights into important environmental factors driving the distribution of
82 individual targets, which may, in turn, improve PFT parameter settings in DGVMs.
83 Comparative studies that evaluate the present-day PFT distributions of DGVMs in a systematic manner, with
84 reference to a field-based evaluation dataset, are so far lacking. In this study, we evaluate representations of
85 vegetation, translated to PFT profiles, obtained by the three different methods (DGVM, RS, DM). We use an
86 independently collected field-based dataset (AR; the Norwegian National map series for Area Resources) for the
87 evaluation. Furthermore, we explore if environmental correlates of vegetation-type distributions identified by DM
88 can be used to improve DGVMs by adjusting parameter settings for high-latitude PFTs.
89 To approach these aims, we constructed a conversion scheme to harmonize the classification schemes of RS, DM
90 and AR into the PFTs used by the DGVM. We represent the vegetation coverage by using plant functional type
91 profiles (PFT profiles), vectors of relative abundances of PFTs within an area, e.g. given study plot, summing to
92 1. We then compare the PFT profiles obtained by DGVM, RS and DM with the AR reference on 20 selected study
93 plots across the Norwegian mainland. Finally, we conduct a series of sensitivity experiments to explore if DGVM
94 performance can be improved by adjusting DGVM parameters for selected environmental drivers.

95 **2 Methods**

96 **2.1 Study area – Norway**

97 The study area covers mainland Norway, spanning latitudes from 57°57'N to 71°11'N and longitudes from 4°29'E
98 to 31°10'E. Norway is characterized by a gradient from a rugged terrain with deep valleys and fjords in the western,
99 oceanic parts to gently undulating hills and shallow valleys in the central and eastern, more continental parts.
100 Temperature and precipitation show considerable variation with latitude, distance from the coast and altitude
101 (Førland, 1979). While the mean annual precipitation ranges from 278 mm in the central inland of S Norway to
102 more than 5000 mm in mid-fjord regions along the western coast, the yearly mean temperature ranges from 7°C
103 in the southwestern lowlands to -4°C in the high mountains (Hanssen-Bauer et al., 2017).

104 The vegetation of Norway is structured along two main climatic gradients; related to temperature/growing-season
105 length and humidity/oceanicity (Bakkestuen et al., 2008). Broadleaf deciduous forests, regularly found in the
106 southern and southwestern parts (the boreonemoral bioclimatic zone), are further west and north (in the southern
107 boreal zone) restricted to locally warm sites (Moen, 1999). With declining temperatures northwards and towards
108 higher altitudes, i.e. in the southern and middle boreal zones, evergreen coniferous boreal forests dominate. In the
109 northern boreal zone they pass gradually into subalpine birch forests which form the tree line in Norway. A total
110 of about 38% of mainland Norway is covered by forests, and about 37% of the land is situated above the forest
111 line (of which two thirds is covered by alpine mountain heaths). Wetlands cover approximately 9% and broadleaf
112 deciduous forests about 0.4% of the land area (Bryn et al., 2018).

113 **2.2 The AR reference dataset**

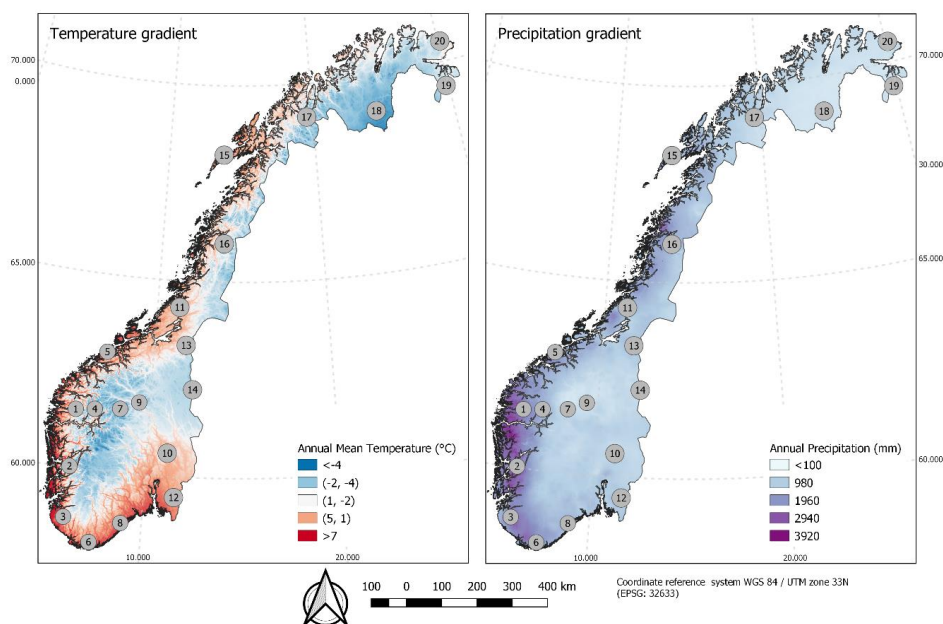
114 Data obtained by in-situ field mapping, which is considered among the most reliable sources of land-cover
115 information (Alexander and Millington, 2000), is practically and economically impossible to obtain for large land



116 areas such as countries (Ullerud et al., 2020). Area-frame surveys based upon stratified statistical sampling may,
117 however, provide accurate, area-representative, homogeneous and unbiased land-cover and land-use data for large
118 areas. To evaluate the three methods for representing vegetation addressed in this study, we used the ‘Norwegian
119 land cover and land resource survey of the outfields’ (*Arealregnskap for utmark*) dataset (Strand, 2013), a
120 Norwegian implementation of the mapping program LUCAS (Eurostat, 2003). Data were collected in the period
121 between 2004–2014 in a systematic 18×18 km grid of 1081 rectangular plots (each 0.6×1.5 km, i.e. 0.9 km²) (Bryn
122 et al., 2018; Strand, 2013). In each plot, expert field surveyors performed land-cover mapping by use of a system
123 with 57 land-cover and vegetation-type classes (Bryn et al., 2018), mapped at a scale of 1:25 000. The data were
124 provided in vector format with vegetation-type attributes assigned to each mapped polygon.

125 2.3 Study plots

126 Twenty out of the 1081 rectangular AR plots were selected to make up our reference dataset, AR (Fig. 1; center
127 coordinates in Table S1). The AR plots spanned elevations from 88 to 1670 m a.s.l., with mean annual temperatures
128 between -4.0°C and 7.1°C and mean annual precipitation between 466 and 2661 mm (Table S1). A test showed
129 that the selection of plots were acceptable representative for bioclimatic variation in Norway (see Fig. S3 and Fig.
130 S4). The test was performed using gridded temperature and precipitation data from seNorge2 (Lussana et al.,
131 2018a; Lussana et al., 2018b), interpolated for each plot by kriging in accordance with Horvath et al. (2019).



132

133 **Figure 1 - Locations of the 20 plots across the two main bioclimatic gradients in the study area: temperature (left) and**
134 **precipitation (right). The plots are numbered by longitude from west to east. Exact values of temperature, precipitation**
135 **and altitude for each plot are given in Table S1.**



136 **2.4 Methods for representing vegetation**

137 In this study, we use 'plot' as a collective term for two partly overlapping spatial units: (i) the 0.9-km² rectangles
 138 of the AR of the reference dataset; and (ii) the 1-km² quadrats with the same centerpoint as, and edges parallel to
 139 those of, the AR rectangles. The latter were used for the three methods of DGVM, RS and DM (Fig. S2).

140 Representations of the vegetation of each of these 20 plots were obtained by three different methods: (i) as the
 141 result of single-cell DGVM simulations for each plot; (ii) inferred from an RS vegetation map of the study area;
 142 and (iii) from vegetation-type DM models (Table 1). In order to make the three methods comparable, vegetation
 143 was represented by plant functional type profiles (PFT profiles), obtained by a conversion scheme (Table 2 and
 144 Sect. 2.5). We define a PFT profile as a thematic representation of the land surface in a given plot or a group of
 145 plots, described as a vector of relative PFT abundances, i.e. values that sum up to 1.

146 **Table 1 – Details of each of the presented methods for representing vegetation. DGVM – dynamic global vegetation**
 147 **model, RS – remote sensing, DM – distribution model. PFT – plant functional type, VT – vegetation type.**

	DGVM	RS	DM
Model type	Process-based mechanistic model	Supervised and unsupervised classification	Statistical model
Software / model name and version	Community Land Model 4.5 – CLM4.5-BGCDV	ENVI (image analysis) and ArcGIS (classification)	R version 3.6.2, generalized linear model
Reference	Oleson et al., 2013	Johansen, 2009	Horvath et al., 2019
Thematic resolution	14 PFTs	25 VTs	31 VTs
Spatial resolution (grid cell)	1 km	30 m	100 m

148

149 **2.4.1 The DGVM method**

150 The DGVM employed in this study was the CLM4.5BGCDV (further referred to as DGVM) embedded in NCAR's
 151 Community Land Model version 4.5 (CLM4.5) (Oleson et al., 2013). In DGVM, plant photosynthesis, stomatal
 152 conductance, carbon/nitrogen allocation, plant phenology and multi-layer soil biogeochemistry are described in
 153 accordance with default CLM4.5, while vegetation dynamics (establishment, survival, mortality and light
 154 competition) are handled separately based upon relatively simple assumptions (Oleson et al., 2013). We used
 155 DGVM in the form of single-cell simulations for the 20 plots with grid-cell size set to 1×1 km (Table 1) to simulate
 156 the fractional cover of each PFT. All models were run with default CLM4.5 values for surface parameters (e.g.
 157 soil texture and depth), with prescribed atmospheric forcing derived from the 3-hourly hindcast of the regional
 158 model (SMHI-RCA4) for the European Domain of the Coordinated Downscaling Experiment – CORDEX for
 159 1980–2010 (Dyrredal et al., 2018). The CORDEX model simulation was used because it has a higher spatial
 160 resolution than the default atmospheric forcing used in CLM4.5 (0.11°×0.11° and 0.5°×0.5°, respectively). An
 161 inspection of the choice of atmospheric forcing, by which the CORDEX data were compared with the SeNorge
 162 data used for DM, showed minimal differences (Fig. S5). Only results obtained using CORDEX data are therefore
 163 shown in this paper.

164 The model was run with default PFT parameters (Table S6). Among the 15 PFTs used in CLM4.5 to represent
 165 vegetated surfaces globally (Lawrence and Chase, 2007), only six (plus bare ground) were relevant for our study
 166 area (Table 2). Bare ground was predicted to occur where plant productivity was below a threshold value
 167 (Dallmeyer et al., 2019). The DGVM simulates the vegetated landunit only (non-grey boxes in Fig. S7) while other
 168 landunits within the 20 plots, including glaciers, wetlands, lakes, cultivated land and urban areas, make up the
 169 “EXCL” PFT category (Table 2). We obtained PFT profiles for each plot by excluding the EXCL category and
 170 recalculating fractions of the vegetated land unit covered by each PFT. Each model simulation was spun-up for



171 400 years to establish a vegetation in equilibrium with the current climate after initialization from bare ground. A
 172 20-year average at the end of the spin-up was used as input for calculation of PFT profiles.

173 **2.4.2 The RS method**

174 As RS product we used SatVeg (Johansen, 2009), a vegetation map for Norway with 25 land-cover classes and a
 175 spatial resolution (pixel size) of 30 m (Table 1). SatVeg is obtained by a combination of unsupervised and
 176 supervised classification methods, applied to Landsat 5/TM and Landsat 7/ETM+ images within the near-infrared
 177 and mid-infrared spectrum. Only pixels that were within each 1-km² plot with majority of their area were taken
 178 into consideration for further calculations.

179 **2.4.3 The DM method**

180 The distribution models (DMs) for 31 vegetation types (VT) obtained by Horvath et al. (2019) using generalized
 181 linear models (GLMs, with logit link and binomial errors, i.e. logistic regression), were used for this study. The
 182 DMs were obtained by using wall-to-wall data for 116 environmental variables, gridded to a spatial resolution of
 183 100×100 m (Table 1) as predictors. All DMs were evaluated by use of an independently collected data set (see
 184 Horvath et al., 2019 for details). A seamless vegetation map (i.e. with one predicted VT for each pixel with no
 185 overlap and no gaps) was obtained from the stack of 31 probability surfaces by assigning to each grid cell the VT
 186 with the highest predicted probability of occurrence within that cell (Ferrier et al., 2002). Pixels that were within
 187 each 1-km² plot with majority of their area were used for further calculations (Fig. S2).

188 **2.5 Conversion to PFT profiles**

189 Harmonisation of the various vegetation classification systems was accomplished by a conversion scheme that
 190 represented each grid cell (RS and DM) or polygon (AR) in each of the 20 plots with one out of the six PFTs
 191 recognised by DGVM (Table 2 and Fig. S2). The scheme was obtained by expert judgements and solicited by a
 192 consensus process which involved ecologists participating in the AR18x18 survey as well as scientists working
 193 with RS and DGVMs.

194 We used the conversion scheme of Table 2 to generate wall-to-wall PFT maps from the original RS, DM and AR
 195 datasets (Table 1) by assigning one PFT to each 30×30 m grid cell, 100×100 m grid cell or VT polygon,
 196 respectively. PFT profiles for each plot at the same thematic resolution as for DGVM were obtained as the vector
 197 with fractions of grid cells or polygons assigned to each of the six PFTs. 'EXCL' classes not represented in DGVM
 198 (cf. Table 2) were left out in order to minimise effects of land use, which could otherwise have brought about
 199 differences in PFT profiles among the compared methods. PFT profiles were obtained for each combination of
 200 method and plot. Aggregated PFT profiles were obtained by averaging the 20 PFT profiles obtained for each
 201 method.

202

203 **Table 2– Conversion scheme for harmonizing vegetation and land cover types across methods (RS, DM and AR) into**
 204 **plant functional types (PFTs). DGVM – dynamic global vegetation model, RS – remote sensing, DM – distribution**
 205 **model. PFT – plant functional type, VT – vegetation type.**

DGVM		RS	DM	AR
PFT code	plant functional type	vegetation / land cover type – remote sensing	vegetation type – distribution model	vegetation type – area frame survey



BG	Bare ground	Exposed alpine ridges, scree and rock complex	Frozen ground, leeward	Frozen ground, leeward
			Frozen ground, ridge	Frozen ground, ridge
			Boulder field	Sand dunes and gravel beaches
			Exposed bedrock	Pioneer alluvial vegetation
				Barren land
				Boulder field
Boreal NET	Boreal needleleaf evergreen tree	Coniferous forest – dense canopy layer	Lichen and heather pine forest	Lichen and heather pine forest
		Coniferous forest and mixed forest - open canopy	Bilberry pine forest	Bilberry pine forest
		Lichen rich pine forest	Lichen & heather spruce forest	Meadow pine forest
			Bilberry spruce forest	Pine forest on lime soils
			Meadow spruce forest	Lichen & heather spruce forest
			Damp forest	Bilberry spruce forest
			Bog forest	Meadow spruce forest
				Damp forest
Temperate BDT	Temperate broadleaf deciduous tree	Low herb forest and broadleaved deciduous forest	Poor / Rich broadleaf deciduous forest	Poor broadleaf deciduous forest
				Rich broadleaf deciduous forest
Boreal BDT	Boreal broadleaf deciduous tree	Tall herb - tall fern deciduous forest	Lichen and heather birch forest	Lichen and heather birch forest
		Bilberry- low fern birch forest	Bilberry birch forest	Bilberry birch forest
		Crowberry birch forest	Meadow birch forest	Meadow birch forest
		Lichen-rich birch forest	Alder forest	Birch forest on lime soils
			Pasture land forest	Alder forest
			Poor / rich swamp forest	Pasture land forest
Boreal BDS	Boreal broadleaf deciduous shrub	Heather-rich alpine ridge vegetation	Lichen heath	Lichen heath
		Lichen-rich heathland	Mountain avens heath	Mountain avens heath
		Heather- and grass-rich early snow patch communities	Dwarf shrub / Alpine calluna heath	Dwarf shrub heath
		Fresh heather and dwarf-shrub communities (u/l)	Alpine damp heath	Alpine calluna heath
			Coastal heath / Coastal calluna heath	Alpine damp heath
			Damp heath	Flood-plain shrubs
				Coastal heath
				Coastal calluna heath
C3	C3 grass	Graminoid alpine ridge vegetation	Moss snowbed / Sedge and grass snowbed	Moss snowbed
		Herb-rich meadows (up-/lowland)	Dry grass heath	Sedge and grass snowbed
		Grass and dwarf willow snow-patch vegetation	Low herb / forb meadow	Dry grass heath
				Low herb meadow
				Low forb meadow
EXCL	Excluded	Ombrotrophic bog and low-grown swamp vegetation	Bog / Mud-bottom fen and bog	Bog
		Tall-grown swamp vegetation	Deer-grass fen / fen	Deer-grass fen



	Wet mires, sedge swamps and reed beds	Sedge marsh	Fen
	Glacier, snow and wet snow-patch vegetation	Pastures	Mud-bottom fen and bog
	Water		Sedge marsh
	Agricultural areas		Cultivated land
	Cities and built-up areas		Pastures
	Unclassified and shadow affected areas,		Built-up areas
			Scattered housing
			Artificial impediment
			Glaciers and perpetual snow
			Sea and ocean
			Water bodies (fresh)

206

207 2.6 Comparison of PFT profiles

208 Aggregated PFT profiles obtained by each of the DGVM, RS and DM methods were compared with the aggregated
 209 PFT profile of the AR reference dataset by a chi-square test (Zuur et al., 2007).

210 For each plot, the dissimilarity between PFTs profiles obtained by each of the DGVM, RS and DM methods and
 211 the PFT profile of the AR dataset was calculated by using proportional dissimilarity (Czekanowski, 1909):

$$212 d_{hj} = \frac{\sum |y_{hji} - y_{0ji}|}{\sum (y_{hji} + y_{0ji})} = 1 - \frac{2 \sum \min(y_{hji}, y_{0ji})}{\sum (y_{hji} + y_{0ji})}$$

213 where y_{hji} refers to the specific element in a PFT profile vector (the fraction occupied by the PFT in question) given
 214 by method h (DGVM, RS or DM; $h = 1, \dots, 3$; the value $h = 0$ refers to the AR reference dataset), j refers to
 215 sampling unit ($j = 1, \dots, 20$) and i refers to PFT ($i = 1, \dots, 6$). Proportional dissimilarity is the Manhattan measure
 216 standardized by division by the sum of the pairwise sums of variable values (here PFTs). Since the values of each
 217 PFT profile sums to one, the index reduces to

$$218 d_{hj} = 1 - \sum \min(y_{hji}, y_{0ji})$$

219 The proportional dissimilarity index is appropriate for incidence data like PFT abundances, i.e. variables that take
 220 zero or positive values. The index reaches a maximum value of 1 when two objects have no common presences
 221 (here, PFTs present in both compared objects) and ignore joint absences (zeros). We compared pairwise
 222 differences between the proportional dissimilarity values among methods, using a Wilcoxon-Mann-Whitney
 223 paired samples test.

224 All raster and vector operations related to DM, RS and AR were carried out in R (version 3.4.3) (R Core Team,
 225 2019) using packages “rgdal” (Rowlingson, 2019), “raster” (Hijmans, 2019) and “sp” (Pebesma and Bivand,
 226 2005), while graphics are produced using the “ggplot2” package (Wickham, 2016). Statistical analyses were
 227 carried out in R (version 3.4.3), using the “vegan” package (Oksanen et al., 2019). All maps were produced in
 228 QGIS (QGIS Development Team, 2019).

229 3 Results

230 The aggregated PFT profiles for the RS and DM datasets did not differ significantly from those of the reference
 231 AR dataset according to the chi-square test, while a significant difference was found for the DGVM profiles (Table
 232 3). While the proportion of pixels attributed to the PFT ‘boreal NET’ by the RS and DM methods underestimated
 233 AR values by 3.0 and 2.8 percentage points, respectively, DGVM overestimated the proportion of boreal NET by

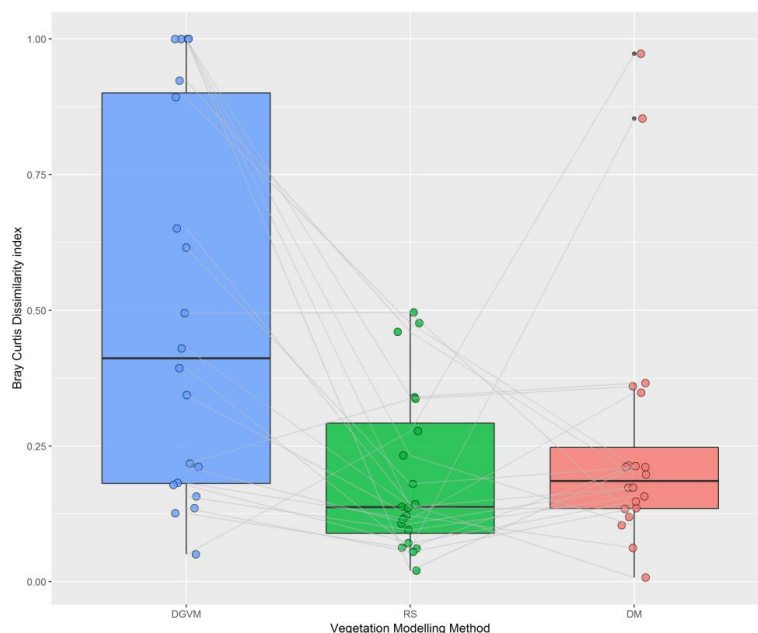


234 20.4 percentage points compared to the AR reference. Also, unproductive areas (BG) were overrepresented by
 235 DGVM (by 16.6 percentage points), less so by RS (4.0 percentage points), while this PFT was slightly
 236 underrepresented by DM (by 5.0 percentage points). Discrepancies were also observed for the cover of the C3
 237 PFT, which was overestimated by RS and DM (by 7.2 and 2.9 percentage points, respectively) and underestimated
 238 by 3.0 percentage points by DGVM. Furthermore, DGVM overestimated BG and temperate BDT cover on the
 239 expense of boreal BDT and boreal BDS.

240 **Table 3 - PFT profiles (columns) aggregated across all 20 plots for the three methods compared in this study and the**
 241 **AR reference dataset. Results of comparisons of aggregated PFT profiles for each of the three methods with the**
 242 **reference are also given. DGVM – dynamic global vegetation model, RS – remote sensing, DM – distribution model, AR**
 243 **– reference dataset. BG – bare ground, boreal NET – boreal needleleaf evergreen trees, temperate BDT – temperate**
 244 **broadleaf deciduous trees, boreal BDT – boreal broadleaf deciduous trees; boreal BDS - boreal broadleaf deciduous**
 245 **shrub, C3 – C3 grasses.**

PFT	Compared methods			Reference
	DGVM (%)	RS (%)	DM (%)	AR (%)
BG	29.5	17.0	7.9	12.9
Boreal NET	57.2	34.0	33.8	36.8
Temperate BDT	5.6	2.0	0.2	0.5
Boreal BDT	3.1	12.5	17.2	15.5
Boreal BDS	4.1	23.8	34.5	30.8
C3	0.5	10.7	6.4	3.5
Chi-square test	$\chi^2= 45.98$, df = 5, p < 0.05	$\chi^2= 6.36$, df = 5, p = 0.27	$\chi^2= 2.61$, df = 5, p = 0.75	

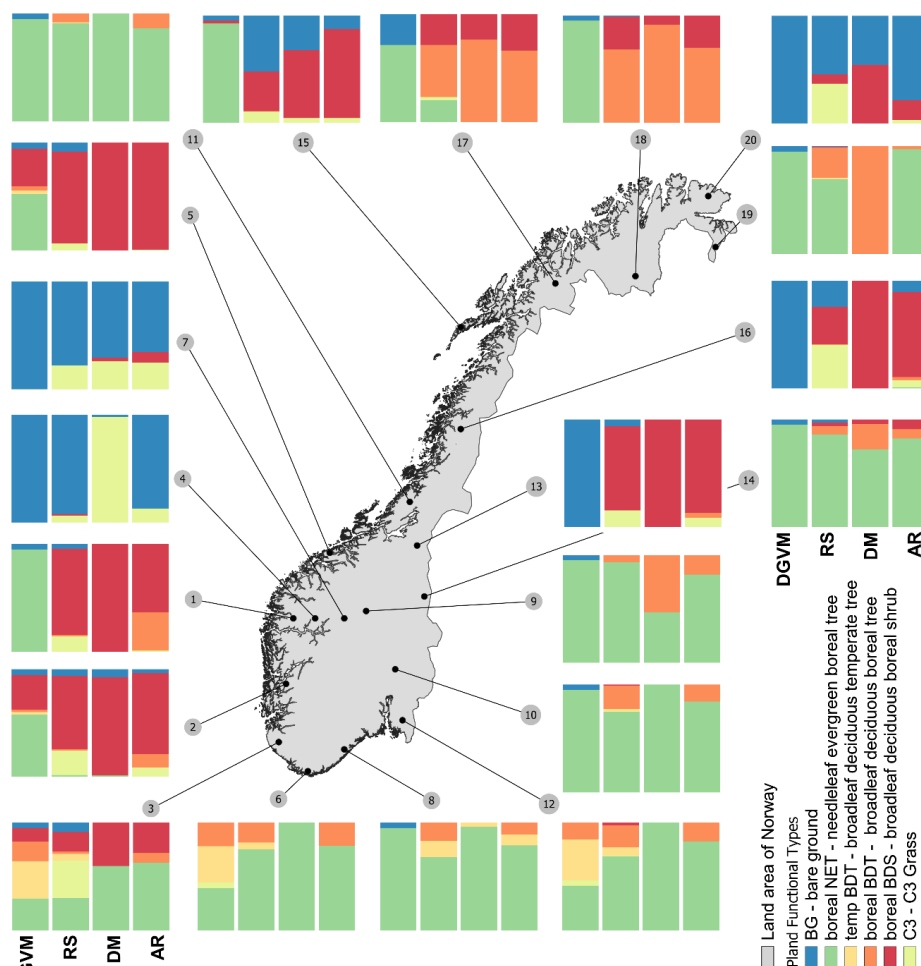
246
 247 In accordance with results from comparisons between aggregated PFT profiles obtained by the three methods and
 248 those obtained for the reference dataset, DGVM profiles for individual plots were significantly more dissimilar to
 249 the AR reference than were RS and DM profiles (Fig. 2). While RS had the lowest median proportional
 250 dissimilarity with the AR reference (0.19, compared to 0.26 for DM and 0.41 for DGVM), DM had the lowest
 251 spread of dissimilarity values, measured as interquartile difference (0.12, compared to 0.19 for RS and 0.72 for
 252 DGVM), among the three methods (Fig. 3). While no dissimilarity value for RS was above 0.50, two sampling
 253 units (4, 19) acted as strong outliers in the distribution of DM values (cf. Fig. 2 and Fig. 3). A comparison of
 254 proportional dissimilarity between pairs of methods revealed significant differences between DGVM profiles and
 255 those obtained by RS and DM (Wilcoxon rank-sum tests: $W = 111$, $p = 0.0167$; and $W = 88$, $p = 0.0026$,
 256 respectively), while RS and DM profiles were not significantly different from each other (Wilcoxon rank-sum test:
 257 $W = 161$, $p = 0.3013$).



258

259 **Figure 2 - Proportional dissimilarity values between PFT profiles for each combination of 20 plots and one of the three**
260 **methods compared in this study, and the corresponding plot in the AR reference dataset. The thick horizontal line, the**
261 **box and the whiskers represent the median, the interquartile difference and the range of values for each method.**

262 Visual inspection of spatial patterns of PFT profile characteristics across the 20 plots suggests that the best
263 agreement among the methods was obtained for the southeastern part of the study area, dominated by the boreal
264 NET (Fig. 3). Compared to the AR reference dataset, PFT profiles obtained by DGVM were strongly biased: in
265 the north (plots 17 and 18) towards boreal NET on the cost of boreal BDT, near the west coast (1, 2, 5 and 15)
266 towards boreal NET on the cost of boreal BDS, and in southern coastal areas (3, 6 and 12) towards temperate BDT
267 instead of boreal NET. In sampling units 13 and 16 DGVM failed to establish vegetation (predicting bare ground)
268 where AR reported boreal BDS. RS represented the PFT profiles of the AR reference well in most cases but tended
269 to overestimate the frequency of dominance by C3 grasses at several locations (plots 3, 16 and 20). While DM
270 showed no general spatial pattern of PFT profile deviations from the reference dataset, PFT profiles of plots 4 and
271 19 obtained by DM had almost no similarity to the corresponding profiles of the AR reference dataset: C3 grasses
272 and boreal BDT were predicted instead of bare ground and boreal NET, respectively.



273
 274 **Figure 3 – PFT profiles for each of the 20 plots for the three methods compared in this study and the AR reference**
 275 **dataset. The columns in each cluster of four bar-charts represent, from left to right, the methods dynamic global**
 276 **vegetation model (DGVM), remote sensing (RS) and distribution model (DM), with the AR reference dataset to the**
 277 **right.**

278 **4 Sensitivity experiments and model improvement**

279 **4.1 Methods**

280 We used the results of PFT profile comparisons between DGVM and the AR reference and the results obtained
 281 for the DM dataset as a starting point for exploring possible relationships between the poor performance of DGVM
 282 and DGVM parameter settings. We first identified the three most abundant PFTs (i.e. boreal NET, boreal BDT
 283 and boreal BDS) in our set of plots (Table S4). Thereafter, we identified the major VTs that were translated into
 284 these PFTs to be pine forest, birch forest and dwarf shrub heath, respectively (Table 4). We selected three of the
 285 most important environmental predictors for the distribution of each of these VTs, as identified by DMs (see
 286 Horvath et al. 2019) for sensitivity experiments of DGVM parameter settings (Table 4): snow water equivalent in



287 October (swe_10), minimum temperature in May (tmin_5) and precipitation seasonality (bioclim_15). We used
288 frequency-of-presence plots (i.e. graphs showing variation in the abundance of the VT as a function of an
289 environmental variable) to identify threshold values for presence of the three VTs and implemented these threshold
290 values into DGVM as new limits for establishment of the three PFTs as shown in Table 4 (also see Fig S11).
291 We explored the extent to which revised parameter settings improved the performance of DGVM on the subset of
292 six plots (i.e. numbers 1, 2, 5, 15, 17 and 18) in which the boreal NEB was most strongly overrepresented compared
293 to the AR reference dataset. Sensitivity experiments were carried out by a stepwise process, in each step adding
294 one new threshold, specific for the three PFTs at the same time. Parameters were added in the following order:
295 swe_10, tmin_5 and bioclim_15 (only relevant for the boreal NET). Only the results of DGVMs with all three
296 parameters changed are reported here (results of the other two experiments are summarised in Table S12). For
297 example, in the three sensitivity model runs (i–iii), (i) the requirement for establishment of boreal NET was set to
298 swe_10 > 150 mm; in (ii) and (iii) the additional demands tmin_5 > -5 °C and bioclim_15 < 50, respectively, were
299 enforced.

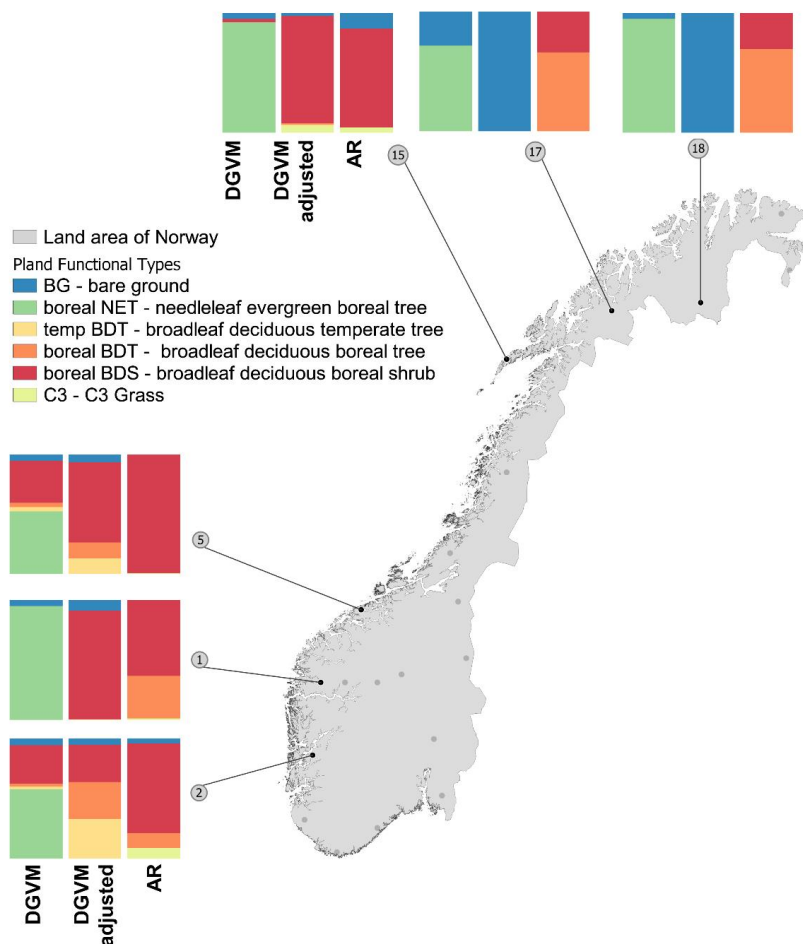
300 **Table 4 – New parameter thresholds for establishment of the three PFTs explored in DGVM sensitivity experiments.**
301 **Variables for which parameter settings were explored were: swe_10 – snow water equivalent in October given in mm;**
302 **tmin_5 – minimum temperature in May (°C); bioclim_15 – precipitation seasonality (unitless index representing annual**
303 **trends in precipitation).**

VT	PFT	SWE_10 (mm)	Tmin_5 (°C)	Bioclim_15
2ef – Dwarf shrub heath / Alpine calluna heath	Boreal broadleaf deciduous shrub	> 380	> -10	–
4a – Lichen and heather birch forest	Boreal broadleaf deciduous tree	> 180	> -7.5	–
6a – Lichen and heather pine forest	Boreal needleleaf evergreen tree	> 150	> -5	< 50

304

305 4.2 Results

306 Adding new parameter thresholds in accordance with Table 4 made PFT profiles identified by DGVM more similar
307 to those of the AR reference dataset for four out of the six plots in the experimental subset (1, 2, 5 and 15): in plots
308 1 and 15, Boreal NET was correctly replaced by boreal BDS; in plots 2 and 5 boreal NET was replaced by boreal
309 BDT, BDS and temperate BDT. Addition of new parameter thresholds also reduced the modelled abundance of
310 boreal NET in plots 17 and 18, but DGVM failed to populate these plots with another PFT (Fig. 4). The improved
311 performance of DGVM on the experimental sampling units was mainly due to the implementation of the threshold
312 for bioclim_15, while the changes made for swe_10 and tmin_5 had little impact on the results (Table S12).



313

314 **Figure 4 – PFT profiles for the subset of six plots subjected to sensitivity experiments with new DGVM establishment**
 315 **thresholds. The columns in each cluster of three bar-charts represent, from left to right, dynamic global vegetation**
 316 **model (DGVM) with original (default) parameter settings, DGVM with revised parameter settings, and the AR**
 317 **reference dataset. For further details, see Table S12.**

318 5 Discussion

319 5.1 Comparison of PFT profiles

320 The maps of PFT distributions generated by DM and RS are generally similar (Fig. S8) across most of our study
 321 area. This indicates that output from DM, which is rarely used for evaluating PFT distributions from DGVMs, can
 322 be used for this purpose in addition to the commonly used RS-based datasets. There are, however, some differences
 323 between results obtained by the two methods near the northern Norwegian coast and in the mountain areas of
 324 western Norway which will be discussed below.

325 We recognise six possible explanations for the differences in PFT profiles obtained by DGVM, RS and DM for
 326 the 20 plots (see Table 5), related to the following issues: (i) the conversion scheme (ref. Table 2); (ii) what is



327 actually modelled by DGVM, RS and DM, e.g. in terms of potential vs actual vegetation; (iii) the performance of
328 individual DM models; (iv) transforming predictions from single DMs into a seamless vegetation map, i.e. that
329 assigns one VT to each pixel; (v) DGVM performance; and (vi) missing PFTs in DGVM.

330 **5.1.1 The conversion scheme**

331 The conversion schemes used to reclassify vegetation and land cover classes into PFTs have been reported as a
332 possible attributor to erroneous PFT distributions (Hartley et al., 2017). While we use a simple conversion scheme
333 which assigns each land cover type/vegetation type to one and only one PFT (Dallmeyer et al., 2019), more
334 complex conversion schemes exist, by which each land cover class is translated into a multi-PFT composition that
335 co-occur within a grid cell (Bonan et al., 2002; Li et al., 2016; Poulter et al., 2011; Poulter et al., 2015). Our
336 approach may be advantageous when the classes to be converted are homogeneous, in the sense that one PFT is
337 clearly dominating in the type, and in the sense that the range of variation within the class in PFTs is negligible,
338 such as is the case for 90% of the DM- and RS-classes in our study. Our simple scheme may, on the other hand,
339 be a source of bias when quantitatively important VTs are ambiguous in one way or the other, or, more commonly,
340 in both ways at the same time. The set of VTs used in our study includes several relevant examples: VTs that may
341 include a wide spectre of tree-dominant types; the VT '*1a/1b - Moss snowbed / Sedge and grass snowbed*' which
342 covers a range of variation in the relative abundance of graminoids and, hence, shows affinity to C3 as well as to
343 BG; and the VT '*8a - Damp forest*', which is usually dominated by the evergreen Scots pine and converted into
344 boreal NET, but that in some instances (e.g. after clear-cutting) is dominated by deciduous trees like *Betula* spp.
345 and should then be converted into boreal BDT (Bryn et al., 2018). However, a close inspection of DM shows that
346 our method reproduces similar PFT profiles as the reference dataset for all plots except two out of 20 plots (the
347 two outliers on Fig. 2, represented by plots 4 and 19 in Fig. 3).

348 In our case, a more complicated conversion scheme is likely to be compensated for by the sub-grid complexity
349 introduced in the process by which PFT profiles are obtained. Rather than estimating a PFT profile for the 1-km²
350 plot directly, i.e. in one operation as in DGVM, the RS-based classes and VTs are first converted into PFTs in their
351 original resolution, and then subsequently subjected to aggregation to obtain the PFT profiles. This results in a
352 sub-grid PFT heterogeneity that could otherwise be implemented by using a more complex conversion scheme.

353 **5.1.2 What is modelled by DGVM, RS and DM**

354 The methods used in this study produce different representations of the vegetated land surface in terms of actual
355 or potential natural vegetation (Table 5). In order to model future vegetation changes and feedbacks, functional
356 type-based models like DGVM implicitly address the processes that control the distribution of vegetation (Bonan
357 et al., 2003; Song et al., 2013). Simulating natural vegetation processes under a given climatic equilibrium scenario
358 (at any given time), DGVM produces a model of potential natural vegetation (ex. Bohn et al., 2000, Hengl et al.
359 2018). RS-based classifications, on the other hand, describe the land surface at a specific time-point or changes
360 through time (e.g. Arctic greening and browning) (Myers-Smith et al., 2020) and, accordingly, portrays actual
361 vegetation as influenced by previous and ongoing land use (Bryn et al., 2013). Depending on the modelling setup,
362 DM may pragmatically describe the current ecological envelope of a target or aim at revealing the proximate
363 causes for its distribution (Ferrier and Guisan, 2006), thus modelling either actual or potential natural vegetation,
364 depending on the input data used for modelling (Hemsing and Bryn, 2012; Hengl et al., 2018).



365 In this study, we carefully restricted our attention to PFTs that represent natural vegetation, excluding VTs with
366 strong anthropogenic influences. This was done for all methods and the AR reference. Nevertheless, differences
367 with respect to what is actually modelled by the different methods, potential vegetation by DGVM and actual
368 vegetation by RS and DM, may have contributed to the observed among-model differences in PFT profiles.

369 5.1.3 DM performance

370 While the performance of the DM method is overall good, two plots stand out by PFT profiles that deviate strongly
371 from the AR reference (Fig. 2). For plot 4, the discrepancy is due to VT “1a/1b - Moss snowbed / Sedge and grass
372 snowbed”, which is represented by one of the best performing among the 31 DMs. For this VT, conversion scheme
373 bias is a more likely reason for the deviant PFT profile. For plot 19, boreal BDT is modelled because the VT
374 predicted by DM is “4a – Lichen and heather birch forest”. The fact that the DM for this VT is among the inferior
375 DMs (see the ranking of individual models presented in Horvath et al. (2019)) makes this explanation more likely
376 in this case.

377 5.1.4 Transformation of single-DM predictions into a vegetation map

378 The performance of DM on the particular plots may also be influenced by the method chosen for transforming
379 predictions from one DM for each VT into a seamless vegetation map. Assigning to each grid cell the VT with the
380 highest predicted probability of presence in that cell, which is a commonly used method for this purpose (Ferrier
381 and Guisan, 2006), favours VTs represented by good DMs. This is brought about by good DMs having a
382 distribution of predictions that is more spread out (with larger predictions for the pixels identified as the most
383 favourable cells) than poor DMs (Halvorsen, 2012). Alternative methods for this purpose should be tested in the
384 context of DGVM evaluating.

385 To avoid uncertainties associated with conversion between type systems and perhaps even further improve the
386 performance of DM, we recommend exploring the option of using PFTs directly as targets in DM. Direct modelling
387 of PFTs rather than taking the detour via VT models may reduce the number of environment predictors required
388 (116 layers used in Horvath et al. (2019)) in addition to circumventing the complicated process of modelling
389 thematically narrow vegetation types (VTs). Another potential advantage of modelling PFT targets directly is that
390 the model parameters will then be PFT specific, and not in need of being converted (from VT into PFT).

391 To further reduce the biases and uncertainties of DM-based PFT profiles, we recommend exploring the use of
392 variables derived from RS directly as predictors in DM. Previous studies have shown that RS -based predictors
393 may enhance DM performance on different scales: on vegetation-type level (Álvarez-Martínez et al., 2018); on
394 the habitat-type level (Mücher et al., 2009); and on the PFT level (Assal et al., 2015). Further suggestions for
395 improvement of the methods used in this study are found in Table 5.

396



397 **Table 5 – A summary of the key properties of the three methods compared in this study. DGVM – dynamic global**
 398 **vegetation model, RS – remote sensing, DM – distribution model, AR – reference dataset.**

Key property	Method		
	DGVM	RS	DM
Modelled property	Process-based vegetation model – using on <i>a priori</i> parameterizations	Classification based on satellite imagery (spectral reflectance)	Statistically based model of a target (response) and the environment (predictors)
Main purpose	Feeding vegetation changes into ESM for further quantification of feedbacks between land surface and the atmosphere	Mapping of land cover or land use for descriptive purposes, management or monitoring	Predicting the spatial distribution of a target and/or to summarise its relationship with the environment
Material	Climate forcing, PFT parameters, host model	Satellite imagery in different bands	Presence-absence training data, environmental predictors
Spatial extent	Global to regional (Single-cell tests)	Global to local	Regional to local
Modelling outcome	Potential vegetation	Actual vegetation	Potential or actual vegetation, depending on the training data
Advantages	<ul style="list-style-type: none"> – Addresses the processes – Feedback loops with other Earth system components can be included – Continuous temporal scale of prediction into the future 	<ul style="list-style-type: none"> – Observation-based – High spatial resolution – Good temporal coverage 	<ul style="list-style-type: none"> – Opens for use of proxies for important predictors – May provide insight into drivers of distributions
Disadvantages	<ul style="list-style-type: none"> – Low performance (e.g. compared with RS and DM) as long as the underlying processes are not fully understood and properly parameterised – Parameter intensive 	<ul style="list-style-type: none"> – Data are sensitive to cloud cover and shaded areas – Atmospheric correction needed – Provides limited insight to the processes that regulate the distributions of land cover types – No feedback included 	<ul style="list-style-type: none"> – Provides limited insight to the processes that regulate the distributions of targets – Temporally static (one time-point addressed by each model) - No feedback included
Possible interactions with the other methods	<ul style="list-style-type: none"> – May improve DM by pointing at relevant predictor variables – May improve RS by identifying threshold values 	<ul style="list-style-type: none"> – May improve DGVM by improved parameterization (based on RS indices) – May improve DM by providing predictor variables, directly or as indices (NDVI, PAR etc) 	<ul style="list-style-type: none"> – May improve parameterization and envelope discrimination of DGVM – May improve RS by targeting specific PFTs that have similar reflectance, but different ecology

399

400 5.1.5 DGVM performance

401 Our results show that, for many plots, the PFT profiles simulated by DGVM differs from those of the reference
 402 dataset. According to our results, DGVM overpredicts the coverage of bare ground and boreal NET and
 403 underpredicts the cover of C3 grasses, boreal BDT and boreal BDS. While the AR reference dataset shows that
 404 the northern plots (specifically plots 17 and 18) are covered by mountain birch forest and shrubs (boreal BDT and
 405 boreal BDS), DGVM predicts dominance of boreal NET in these plots. Overestimation of boreal NET has also
 406 been reported by Hickler et al. (2012) for large parts of Scandinavia, who attributed this to the lacking
 407 representation of shade tolerance classes in DGVM models. A similar pattern is seen in our results: the PFT profiles
 408 obtained by DGVM during the 400-year spin-up (Fig. S10) show no sign of boreal BDT in the early phases of
 409 model prediction, as expected of an early successional forest in Norway.

410 The western parts of Scandinavia are dominated by shade intolerant birch forests (Bryn et al., 2018) which
 411 gradually give way to coniferous forests along the oceanicity-continentiality gradient towards east (Wielgolaski,
 412 2005). The overprediction of DGVM in the west indicates that the DGVM does not only lack shade-intolerant
 413 PFTs, but also that improved representation of winter-time respiration loss and soil frost-induced drought stress of



414 boreal NET in spring in regions with higher temperature fluctuations around 0°C during winter time compared to
415 the more continental regions (see e.g. Oksanen, 1995; Sevanto et al., 2006) are needed.
416 Our results further suggest that the DGVM underrepresents grasses and shrubs compared to the reference dataset.
417 This may be explained by the built-in constraints in the light competition scheme of DGVM. For example Oleson
418 et al. (2013) mention that regardless of grass and shrub productivity, trees will cover up to 95% of the land unit
419 when their productivity permits. The priority given to a PFT in DGVM decreases with the stature of the organisms
420 in question because of the increasing probability that a lower layer is covered by another layer. The degree of
421 underrepresentation is therefore expected to increase from shrubs to grasses. Accordingly, DGVM predict
422 dominance by trees in the most productive regions, by grasses in less productive regions, and by shrubs in the least
423 productive non-desert regions (Zeng et al., 2008). The underrepresentation of C3 grasses by DGVM across the 20
424 study plots in our study accords with the results of Zhu et al. (2018), who found that C3 grasses are underpredicted
425 on a global level in an earlier version of DGVM.
426 Inappropriate parameterisation of shrubs may be a reason why the DGVM underestimates boreal BDS in many of
427 the coastal plots (1, 2, 5, 15) (Table S6). The implementation of shrubs as a new PFT in an earlier version of
428 DGVM (CLM3-DGVM) by Zeng et al. (2008), which is parameterised for representation of taller shrubs with
429 heights between 0.1 and 0.5 m, may not suit the majority of dwarf shrubs (of genera *Calluna*, *Betula*, *Empetrum*)
430 that abundantly occurs in Norwegian ecosystems. To this, Castillo et al. (2012) add that the sparse shrub and grass
431 vegetation cover simulated by DGVM in the tundra regions may be caused by the soil moisture bias inherited from
432 the host land model CLM4 (Lawrence et al., 2011). Another reason for DGVM's underestimation of boreal BDS
433 in coastal areas could be the 4000-yr tradition of coastal heath management in Norway (Bryn et al., 2010) which
434 causes a large discrepancy between the actual vegetation modelled by RS, DM and AR and the potential natural
435 vegetation simulated by DGVM under present-day climatic conditions (e.g. Bohn et al., 2000, Hengl et al. 2018).
436 We therefore argue that more sensitivity studies of PFT-specific parameters for height, survival, establishment
437 etc., across all PFTs, are needed.
438 Despite the shortcomings discussed above, DGVM performs reasonably well for some PFTs. One example is the
439 temperate BDT, which is correctly predicted by the model to be restricted to the southern coastal plots (Bohn et
440 al., 2000; Moen, 1999). This finding suggests that some climatically driven PFTs (i.e. temperate BDT) are well
441 implemented by the existing parameters in the current DGVM.

442 5.1.6 Missing PFTs

443 DGVM coerces the World's immense variation in plant species composition (vegetation) into a very limited
444 number of predefined PFTs, compared to classification schemes used by the other methods in this study (RS, DM
445 and AR; see Table 2) and by other approaches to systematisation of ecodiversity (e.g. Dinerstein et al., 2017; Keith
446 et al., 2020). In particular, the number of high-latitude specific PFTs is insufficient to realistically represent the
447 biodiversity of these ecoregions, as pointed out by Bjordal (2018) and Vowles & Björk (2017). Comparisons
448 between PFT profiles obtained by DGVM and profiles obtained by DM may suggest specific vegetation types that
449 need to be better represented in DGVMs, either by improving an existing PFT or by adding a new PFT (e.g. dwarf
450 shrub vs. tall shrub; moss dominated snow-beds, wetlands, lichens). In our study, the PFT profile of DGVM is
451 represented by the six boreal PFTs, whereas the original data for RS, DM and AR include an average of 17% (ref.
452 Table S4) of the total area which cannot be represented by these six PFTs (classes for "Excluded" PFT category



453 ref. Table 2). This reminds us of the missing PFTs in the classification scheme of the DGVM, but it also points to
454 the problem that certain ecosystems in our study area do not have a real representation in the PFT schemes of
455 DGVM. This is exemplified by wetlands; important ecosystems that are still not represented in many of the current
456 DGVMs. This is not only problematic from the perspective of land surface energy balance (Wullschleger et al.,
457 2014), but also brings issues of carbon storage and cycling, and other interactions between the land surface and
458 the atmosphere (Bjorndal, 2018).

459 Our results demonstrate a great potential for increasing the thematic resolution of DGVMs in terms of developing
460 and parameterizing new specific PFTs to be representative of the high-latitude and high-altitude habitats, as
461 exemplified by Druel et al. (2017) and also deriving parameters from observations, DMs or RS products (Bjorndal,
462 2018; Wullschleger et al., 2014), specific for the high latitudes (Druel et al., 2017).

463 5.2 Sensitivity tests

464 Adjusting DGVM parameters so that they correspond better with environmental drivers known to be functional in
465 the high-latitude PFTs has been suggested as a measure to improve the performance of DGVM in these parts of
466 the World (Wullschleger et al., 2014). Our simple sensitivity experiments demonstrate that DM results can inform
467 parameterisation, in DGVM, of the range along variables used in DM where a PFT occurs. Most notably, we
468 recognized three important environmental drivers for the distribution of high-latitude PFTs not yet represented
469 well in DGVM. This adds to environmental thresholds for establishment, survival or mortality of a PFT previously
470 used in DGVMs to restrict the predicted distribution of PFTs to realistic geographic regions (Miller and Smith,
471 2012).

472 Adjustment of the climatic thresholds for the establishment of the high-latitude PFTs (i.e. boreal NET, BDT, BDS)
473 seemingly bring the PFT profiles of DGVM closer to those of the reference data (Fig. 4). In particular, the
474 sensitivity experiments with DGVM highlight the importance of precipitation seasonality (i.e. bioclim_15) as a
475 critical limiting factor for the establishment of boreal NET. While some studies have emphasized the importance
476 of seasonal distribution of rainfall on vegetation in the semi-arid areas (Zhang et al., 2018), the importance of this
477 factor for high-altitude areas is less well studied (Oksanen, 1995; Sevanto et al., 2006). Better representation of
478 the processes related to the response of boreal NET to water availability, especially spring-drought in DGVM, also
479 warrants further investigation. From our results for Sites 17 and 18, we notice that adjusting the climatic thresholds
480 for growth of boreal NET does not automatically make other PFTs grow. Boreal BDT and BDS can establish at
481 both sites, but their growth rates are too slow to make them occupy a large area at these sites. This prevents
482 development of similarity with the PFT profiles of AR reference dataset (Fig. 4) and implies that other
483 environmental conditions, e.g., nitrogen availability, might play a more important role in limiting the growth of
484 BDT and BDS in CLM4.5BGCDV. The biases of DGVMs in simulating boreal broadleaf deciduous tree and shrub
485 has been widely noticed in other studies (Castillo et al., 2012), and should be investigated further.

486 While going into further details of which additional PFTs should be included in DGVMs and how these and other
487 PFTs should be parameterised is beyond the scope of the present paper, we emphasize the potential of using DM
488 for improving the parameters of DGVMs. More specifically, we propose more intensive exploration of DM as a
489 tool for identification of potential environmental drivers for the high-latitude PFTs, which may enhance the
490 performance of DGVMs in high-latitude ecoregions.



491 **6 Conclusions**

492 This study emphasizes the potential of using distribution models (DM) for representing present-day vegetation in
493 evaluations of plant functional type (PFT) distributions simulated by dynamic global vegetation models (DGVMs)
494 and for improvement of specific PFT parameters within DGVMs. By identification of the main differences among
495 PFT profiles obtained by three methods (DGVM, RS and DM) in selected high-latitude plots distributed across
496 climatic gradients in Norway, we show that PFT profiles derived from DM and RS are in the same range of
497 reliability, judged by resemblance to a reference dataset (AR). Hence, we suggest that DM results can be used as
498 a complementary evaluation dataset to benchmark the present-day DGVMs. This approach is recommended when
499 high-quality RS products are not available.

500 Comparing the twenty PFT profiles obtained by DGVM with those obtained by AR shows a large overestimation
501 by DGVM of boreal needleleaf evergreen trees (boreal NET) and bare ground at the expense of boreal broadleaf
502 deciduous trees and shrubs. This is attributed to missing processes and PFT parameterizations of high-latitude
503 PFTs in DGVM. We use DM results to identify three new PFT-specific environmental parameters which, in a
504 series of sensitivity experiments, improve the distribution of boreal NET predicted by DGVM. The new PFT-
505 specific thresholds for establishment decrease the bias of boreal NET in DGVM across four out of six plots. We
506 argue that these new thresholds should be transferable to other DGVMs simulating high-latitude PFTs, and that
507 our DM-based approach can be transferred to other ecosystems.

508 Further development of DGVM, such as refining parameters for existing boreal PFTs and increasing the thematic
509 resolution of PFTs for boreal areas, should be strongly encouraged to achieve a more realistic simulation of the
510 distribution of actual vegetation by DGVM, to increase the reliability of future predictions, and the reliability of
511 predicted vegetation feedbacks in the climate system.

512 **7 Acknowledgements**

513 NIBIO is acknowledged for providing access to the area-frame survey AR18X18 dataset. UNINET Sigma2 is
514 acknowledged for providing computing facilities. Geir-Harald Strand is acknowledged for providing scientific
515 assistance and Michal Torma for providing technical assistance.

516 **8 Data availability.**

517 The scripts used in this study are available in the GitHub repository https://github.com/geconhm/DGVM_RS_DM_Norway. High-resolution DM-based and RS-based PFT maps are available from the
518 authors on request (Fig. S8). DGVM outputs are provided in the Table S9, Table S12 and Fig. S10.

520 **9 Author contributions.**

521 All authors have contributed to conceptualizing the research idea. PH curated the data and was responsible for the
522 distribution modelling and for compiling and analysing the data from all methods. HT carried out the modelling
523 and sensitivity tests using the DGVM (CLM4.5-BGCDV). PH together with AB and RH were responsible for
524 writing, with all authors contributing to reviewing and editing the paper. FS, AB, TKB and LMT acquired funding
525 for this research.



526 **10 Competing interests.**

527 The authors declare that they have no conflict of interest.

528 **11 Financial support.**

529 This work forms a contribution to LATICE (<https://www.mn.uio.no/latice>), which is a Strategic Research Initiative
530 funded by the Faculty of Mathematics and Natural Sciences at the University of Oslo (UiO/GEO103920). It is also
531 part of the EMERALD project (294948) funded by the Research Council of Norway.

532 **12 References:**

533 Alexander, R., and Millington, A. C.: Vegetation mapping: From Patch to Planet, Vegetation Mapping, John Wiley
534 & Sons, LTD, Chichester, England, 321-331 pp., 2000.

535 Álvarez-Martínez, J. M., Jiménez-Alfaro, B., Barquín, J., Ondiviela, B., Recio, M., Silió-Calzada, A., and Juanes,
536 J. A.: Modelling the area of occupancy of habitat types with remote sensing, Methods in Ecology and Evolution,
537 9, 580-593, <https://doi.org/10.1111/2041-210X.12925>, 2018.

538 Assal, T. J., Anderson, P. J., and Sibold, J.: Mapping forest functional type in a forest-shrubland ecotone using
539 SPOT imagery and predictive habitat distribution modelling, Remote Sensing Letters, 6, 755-764,
540 <https://doi.org/10.1080/2150704x.2015.1072289>, 2015.

541 Bakkestuen, V., Erikstad, L., and Halvorsen, R.: Step-less models for regional environmental variation in Norway,
542 J. Biogeogr., 35, 1906-1922, <https://doi.org/10.1111/j.1365-2699.2008.01941.x>, 2008.

543 Bjordal, J.: Potential Implications of Lichen Cover for the Surface Energy Balance: Implementing Lichen as a new
544 Plant Functional Type in the Community Land Model (CLM4.5), Master Thesis, Department of Geosciences,
545 University of Oslo, Oslo, 99 pp., 2018.

546 Bohn, U., Gollub, G., Hettwer, C., Neuhäuslova, Z., Raus, T., Schlüter, H., and Weber, H.: Map of the Natural
547 Vegetation of Europe. Scale 1 : 2 500 000., Federal Agency for Nature Conservation, Münster, 2000.

548 Bonan, G. B., Levis, S., Kergoat, L., and Oleson, K. W.: Landscapes as patches of plant functional types: An
549 integrating concept for climate and ecosystem models, Global Biogeochemical Cycles, 16, 5-1-5-23,
550 <https://doi.org/10.1029/2000gb001360>, 2002.

551 Bonan, G. B., Levis, S., Sitch, S., Vertenstein, M., and Oleson, K. W.: A dynamic global vegetation model for use
552 with climate models: concepts and description of simulated vegetation dynamics, Global Change Biol., 9, 1543-
553 1566, <https://doi.org/10.1046/j.1365-2486.2003.00681.x>, 2003.

554 Bonan, G. B.: Forests, Climate, and Public Policy: A 500-Year Interdisciplinary Odyssey, Annual Review of
555 Ecology, Evolution, and Systematics, 47, 97-121, <https://doi.org/10.1146/annurev-ecolsys-121415-032359>, 2016.

556 Bryn, A., Dramstad, W., Fjellstad, W., and Hofmeister, F.: Rule-based GIS-modelling for management purposes:
557 A case study from the islands of Froan, Sør-Trøndelag, mid-western Norway, Norsk Geografisk Tidsskrift, 64,
558 175-184, <https://doi.org/10.1080/00291951.2010.528224>, 2010.

559 Bryn, A., Dourojeanni, P., Hemsing, L. Ø., and O'Donnell, S.: A high-resolution GIS null model of potential forest
560 expansion following land use changes in Norway, Scand. J. For. Res., 28, 81-98,
561 <https://doi.org/10.1080/02827581.2012.689005>, 2013.

562 Bryn, A., Strand, G.-H., Angeloff, M., and Rekdal, Y.: Land cover in Norway based on an area frame survey of
563 vegetation types, Norsk Geografisk Tidsskrift, 72, 1-15, <https://doi.org/10.1080/00291951.2018.1468356>, 2018.

564 Czekanowski, J.: Zur differentialdiagnose der Neandertalgruppe, Friedr. Vieweg & Sohn, 1909.



- 565 Dallmeyer, A., Claussen, M., and Brovkin, V.: Harmonising plant functional type distributions for evaluating Earth
566 System Models, *Climate of the Past*, 15, 335-366, <https://doi.org/10.5194/cp-15-335-2019>, 2019.
- 567 Davin, E. L., and de Noblet-Ducoudré, N.: Climatic Impact of Global-Scale Deforestation: Radiative versus
568 Nonradiative Processes, *J. Clim.*, 23, 97-112, <https://doi.org/10.1175/2009jcli3102.1>, 2010.
- 569 Dinerstein, E., Olson, D., Joshi, A., Vynne, C., Burgess, N. D., Wikramanayake, E., Hahn, N., Palminteri, S.,
570 Hedao, P., Noss, R., Hansen, M., Locke, H., Ellis, E. C., Jones, B., Barber, C. V., Hayes, R., Kormos, C., Martin,
571 V., Crist, E., Sechrest, W., Price, L., Baillie, J. E. M., Weeden, D., Suckling, K., Davis, C., Sizer, N., Moore, R.,
572 Thau, D., Birch, T., Potapov, P., Turubanova, S., Tyukavina, A., de Souza, N., Pintea, L., Brito, J. C., Llewellyn,
573 O. A., Miller, A. G., Patzelt, A., Ghazanfar, S. A., Timberlake, J., Kloser, H., Shennan-Farpon, Y., Kindt, R.,
574 Lilleso, J. B., van Breugel, P., Graudal, L., Voge, M., Al-Shammari, K. F., and Saleem, M.: An Ecoregion-Based
575 Approach to Protecting Half the Terrestrial Realm, *Bioscience*, 67, 534-545, <https://doi.org/10.1093/biosci/bix014>,
576 2017.
- 577 Druel, A., Peylin, P., Krinner, G., Ciais, P., Viovy, N., Peregon, A., Bastrikov, V., Kosykh, N., and Mironycheva-
578 Tokareva, N.: Towards a more detailed representation of high-latitude vegetation in the global land surface model
579 ORCHIDEE (ORC-HL-VEGv1.0), *Geoscientific Model Development*, 10, 4693-4722,
580 <https://doi.org/10.5194/gmd-10-4693-2017>, 2017.
- 581 Duveiller, G., Hooker, J., and Cescatti, A.: The mark of vegetation change on Earth's surface energy balance,
582 *Nature Communications*, 9, 679, <https://doi.org/10.1038/s41467-017-02810-8>, 2018.
- 583 Dyrddal, A. V., Stordal, F., and Lussana, C.: Evaluation of summer precipitation from EURO-CORDEX fine-scale
584 RCM simulations over Norway, *International Journal of Climatology*, 38, 1661-1677,
585 <https://doi.org/10.1002/joc.5287>, 2018.
- 586 Eurostat: The Lucas Survey: European Statisticians Monitor Territory, Office for Official Publications of the
587 European Communities, Luxembourg, 2003.
- 588 Ferrier, S., Watson, G., Pearce, J., and Drielsma, M.: Extended statistical approaches to modelling spatial pattern
589 in biodiversity in northeast New South Wales. I. Species-level modelling, *Conserv. Biol.*, 11, 2275-2307,
590 <https://doi.org/10.1023/a:1021302930424>, 2002.
- 591 Ferrier, S., and Guisan, A.: Spatial modelling of biodiversity at the community level, *J. Appl. Ecol.*, 43, 393-404,
592 <https://doi.org/10.1111/j.1365-2664.2006.01149.x>, 2006.
- 593 Fisher, R., McDowell, N., Purves, D., Moorcroft, P., Sitch, S., Cox, P., Huntingford, C., Meir, P., and Ian
594 Woodward, F.: Assessing uncertainties in a second-generation dynamic vegetation model caused by ecological
595 scale limitations, *New Phytol.*, 187, 666-681, <https://doi.org/10.1111/j.1469-8137.2010.03340.x>, 2010.
- 596 Franklin, S. E., and Wulder, M. A.: Remote sensing methods in medium spatial resolution satellite data land cover
597 classification of large areas, *Progress in Physical Geography*, 26, 173-205,
598 <https://doi.org/10.1191/0309133302pp332ra>, 2002.
- 599 Førland, E.: Precipitation and topography [in Norwegian with English summary], *Klima*, 79, 23-24, 1979.
- 600 Gotangco Castillo, C. K., Levis, S., and Thornton, P.: Evaluation of the New CNDV Option of the Community
601 Land Model: Effects of Dynamic Vegetation and Interactive Nitrogen on CLM4 Means and Variability, *J. Clim.*,
602 25, 3702-3714, <https://doi.org/10.1175/jcli-d-11-00372.1>, 2012.
- 603 Halvorsen, R.: A gradient analytic perspective on distribution modelling, *Sommerfeltia*, 35, 1-165,
604 <https://doi.org/10.2478/v10208-011-0015-3>, 2012.
- 605 Hanssen-Bauer, I., Førland, E., Haddeland, I., Hisdal, H., Lawrence, D., Mayer, S., Nesje, A., Nilsen, J., Sandven,
606 S., and Sandø, A.: Climate in Norway 2100—A knowledge base for climate adaptation, The Norwegian Centre for
607 Climate Services, The Norwegian Centre for Climate Services, 2017.



- 608 Hartley, A. J., MacBean, N., Georgievski, G., and Bontemps, S.: Uncertainty in plant functional type distributions
609 and its impact on land surface models, *Remote Sens. Environ.*, 203, 71-89,
610 <https://doi.org/10.1016/j.rse.2017.07.037>, 2017.
- 611 Hemsing, L. Ø., and Bryn, A.: Three methods for modelling potential natural vegetation (PNV) compared: A
612 methodological case study from south-central Norway, *Norsk Geografisk Tidsskrift - Norwegian Journal of*
613 *Geography*, 66, 11-29, <https://doi.org/10.1080/00291951.2011.644321>, 2012.
- 614 Henderson, E. B., Ohmann, J. L., Gregory, M. J., Roberts, H. M., and Zald, H.: Species distribution modelling for
615 plant communities: stacked single species or multivariate modelling approaches?, *Applied Vegetation Science*, 17,
616 516-527, <https://doi.org/10.1111/avsc.12085>, 2014.
- 617 Hengl, T., Walsh, M. G., Sanderman, J., Wheeler, I., Harrison, S. P., and Prentice, I. C.: Global mapping of
618 potential natural vegetation: an assessment of machine learning algorithms for estimating land potential, *PeerJ*, 6,
619 e5457, <https://doi.org/10.7717/peerj.5457>, 2018.
- 620 Hickler, T., Vohland, K., Feehan, J., Miller, P. A., Smith, B., Costa, L., Giesecke, T., Fronzek, S., Carter, T. R.,
621 Cramer, W., Kuhn, I., and Sykes, M. T.: Projecting the future distribution of European potential natural vegetation
622 zones with a generalized, tree species-based dynamic vegetation model, *Global Ecol. Biogeogr.*, 21, 50-63,
623 <https://doi.org/10.1111/j.1466-8238.2010.00613.x>, 2012.
- 624 Horvath, P., Halvorsen, R., Stordal, F., Tallaksen, L. M., Tang, H., and Bryn, A.: Distribution modelling of
625 vegetation types based on area frame survey data, *Applied Vegetation Science*, 22, 547-560,
626 <https://doi.org/10.1111/avsc.12451>, 2019.
- 627 Johansen, B. E.: Satellittbasert vegetasjonskartlegging for Norge, Direktoratet for Naturforvaltning, Norsk
628 Romsenter, 2009.
- 629 Keith, D. A., Ferrer, J. R., Nicholson, E., Bishop, M. J., Polidoro, B. A., RamirezLlodra, E., Tozer, M. G., Nel, J.
630 L., Nally, R. M., Greg, E. J., Watermeyer, K. E., Essl, F., Faber-Langendoen, D., Franklin, J., Lehmann, C. E. R.,
631 Etter, A., Roux, D. J., Stark, J. S., Rowland, J. A., Brummitt, N. A., Fernandez-Arcaya, U. C., Suthers, I. M.,
632 Wisser, S. K., Donohue, I., Jackson, L. J., Pennington, R. T., Pettoelli, N., Andrade, A., Kontula, T., Lindgaard,
633 A., Tahvanainen, T., Terauds, A., Venter, O., Watson, J. E. M., Chadwick, M. A., Murray, N. J., Moat, J., Pliscoff,
634 P., Zager, I., and Kingsford, R. T.: The IUCN Global Ecosystem Typology v1.01: Descriptive profiles for Biomes
635 and Ecosystem Functional Groups, IUCN, CEM, New York, 172, 2020.
- 636 Lawrence, D. M., Oleson, K. W., Flanner, M. G., Thornton, P. E., Swenson, S. C., Lawrence, P. J., Zeng, X.,
637 Yang, Z. L., Levis, S., and Sakaguchi, K.: Parameterization improvements and functional and structural advances
638 in version 4 of the Community Land Model, *Journal of Advances in Modeling Earth Systems*, 3,
639 <https://doi.org/10.1029/2011MS00045>, 2011.
- 640 Lawrence, P. J., and Chase, T. N.: Representing a new MODIS consistent land surface in the Community Land
641 Model (CLM 3.0), *Journal of Geophysical Research*, 112, n/a-n/a, <https://doi.org/10.1029/2006jg000168>, 2007.
- 642 Li, W., Ciais, P., MacBean, N., Peng, S., Defourny, P., and Bontemps, S.: Major forest changes and land cover
643 transitions based on plant functional types derived from the ESA CCI Land Cover product, *International Journal of*
644 *Applied Earth Observation and Geoinformation*, 47, 30-39, <https://doi.org/10.1016/j.jag.2015.12.006>, 2016.
- 645 Li, W., MacBean, N., Ciais, P., Defourny, P., Lamarche, C., Bontemps, S., Houghton, R. A., and Peng, S.: Gross
646 and net land cover changes in the main plant functional types derived from the annual ESA CCI land cover maps
647 (1992–2015), *Earth Syst. Sci. Data*, 10, 219-234, <https://doi.org/10.5194/essd-10-219-2018>, 2018.
- 648 Lussana, C., Saloranta, T., Skaugen, T., Magnusson, J., Tveito, O. E., and Andersen, J.: seNorge2 daily
649 precipitation, an observational gridded dataset over Norway from 1957 to the present day, *Earth System Science*
650 *Data*, 10, 235-249, <https://doi.org/10.5194/essd-10-235-2018>, 2018a.
- 651 Lussana, C., Tveito, O., and Uboldi, F.: Three-dimensional spatial interpolation of 2 m temperature over Norway,
652 *Quarterly Journal of the Royal Meteorological Society*, 144, 344-364, <https://doi.org/10.1002/qj.3208>, 2018b.



- 653 Miller, P. A., and Smith, B.: Modelling Tundra Vegetation Response to Recent Arctic Warming, *Ambio*, 41, 281-
654 291, <https://doi.org/10.1007/s13280-012-0306-1>, 2012.
- 655 Moen, A.: Vegetation, Norwegian Mapping Authority, Hønefoss, 200 s. ill. 234 cm pp., 1999.
- 656 Múcher, C. A., Hennekens, S. M., Bunce, R. G. H., Schaminée, J. H. J., and Schaepman, M. E.: Modelling the
657 spatial distribution of Natura 2000 habitats across Europe, *Landscape Urban Plann.*, 92, 148-159,
658 <https://doi.org/10.1016/j.landurbplan.2009.04.003>, 2009.
- 659 Myers-Smith, I. H., Forbes, B. C., Wilmking, M., Hallinger, M., Lantz, T., Blok, D., Tape, K. D., Macias-Fauria,
660 M., Sass-Klaassen, U., Lévesque, E., Boudreau, S., Ropars, P., Hermanutz, L., Trant, A., Collier, L. S., Weijers,
661 S., Rozema, J., Rayback, S. A., Schmidt, N. M., Schaepman-Strub, G., Wipf, S., Rixen, C., Ménard, C. B., Venn,
662 S., Goetz, S., Andreu-Hayles, L., Elmendorf, S., Ravolainen, V., Welker, J., Grogan, P., Epstein, H. E., and Hik,
663 D. S.: Shrub expansion in tundra ecosystems: dynamics, impacts and research priorities, *Environmental Research*
664 *Letters*, 6, 045509, <https://doi.org/10.1088/1748-9326/6/4/045509>, 2011.
- 665 Myers-Smith, I. H., Kerby, J. T., Phoenix, G. K., Bjerke, J. W., Epstein, H. E., Assmann, J. J., John, C., Andreu-
666 Hayles, L., Angers-Blondin, S., Beck, P. S. A., Berner, L. T., Bhatt, U. S., Bjorkman, A. D., Blok, D., Bryn, A.,
667 Christiansen, C. T., Cornelissen, J. H. C., Cunliffe, A. M., Elmendorf, S. C., Forbes, B. C., Goetz, S. J., Hollister,
668 R. D., de Jong, R., Lorant, M. M., Macias-Fauria, M., Maseyk, K., Normand, S., Olofsson, J., Parker, T. C.,
669 Parmentier, F.-J. W., Post, E., Schaepman-Strub, G., Stordal, F., Sullivan, P. F., Thomas, H. J. D., Tømmervik,
670 H., Treharne, R., Tweedie, C. E., Walker, D. A., Wilmking, M., and Wipf, S.: Complexity revealed in the greening
671 of the Arctic, *Nature Climate Change*, 10, 106-117, <https://doi.org/10.1038/s41558-019-0688-1>, 2020.
- 672 Oksanen, L.: Isolated occurrences of spruce, *Picea abies*, in northernmost Fennoscandia in relation to the enigma
673 of continental mountain birch forests, *Acta Bot. Fenn.*, 81-92, 1995.
- 674 Oleson, K. W., Lawrence, D. M., Bonan, G. B., Drewniak, B., Huang, M., Koven, C. D., Levis, S., Li, F., Riley,
675 W. J., Subin, Z. M., Swenson, S. C., and Thornton, P. E.: Technical Description of version 4.5 of the Community
676 Land Model (CLM), NCAR Earth System Laboratory Climate and Global Dynamics Division, BOULDER,
677 COLORADO, USA, 2013.
- 678 Pebesma, E. J., and Bivand, R. S.: Classes and methods for spatial data in {R}, *R News*, 5, 9-13, 2005.
- 679 Poulter, B., Ciais, P., Hodson, E., Lischke, H., Maignan, F., Plummer, S., and Zimmermann, N. E.: Plant functional
680 type mapping for earth system models, *Geoscientific Model Development*, 4, 993-1010,
681 <https://doi.org/10.5194/gmd-4-993-2011>, 2011.
- 682 Poulter, B., MacBean, N., Hartley, A., Khlystova, I., Arino, O., Betts, R., Bontemps, S., Boettcher, M.,
683 Brockmann, C., Defourny, P., Hagemann, S., Herold, M., Kirches, G., Lamarche, C., Lederer, D., Ottlé, C., Peters,
684 M., and Peylin, P.: Plant functional type classification for earth system models: results from the European Space
685 Agency's Land Cover Climate Change Initiative, *Geosci. Model Dev.*, 8, 2315-2328, <https://doi.org/10.5194/gmd-8-2315-2015>, 2015.
- 687 Scheiter, S., Langan, L., and Higgins, S. I.: Next-generation dynamic global vegetation models: learning from
688 community ecology, *New Phytol.*, 198, 957-969, <https://doi.org/10.1111/nph.12210>, 2013.
- 689 Seo, H., and Kim, Y.: Interactive impacts of fire and vegetation dynamics on global carbon and water budget using
690 Community Land Model version 4.5, *Geoscientific Model Development*, 12, 457-472,
691 <https://doi.org/10.5194/gmd-12-457-2019>, 2019.
- 692 Sevanto, S., Suni, T., Pumpanen, J., Grönholm, T., Kolari, P., Nikinmaa, E., Hari, P., and Vesala, T.: Wintertime
693 photosynthesis and water uptake in a boreal forest, *Tree Physiology*, 26, 749-757,
694 <https://doi.org/10.1093/treephys/26.6.749>, 2006.
- 695 Simensen, T., Horvath, P., Erikstad, L., Bryn, A., Vollering, J., and Halvorsen, R.: Composite landscape predictors
696 improve distribution models of ecosystem types, *Divers. Distrib.*, <https://doi.org/10.1111/ddi.13060> accepted.
- 697 Sitch, S., Huntingford, C., Gedney, N., Levy, P. E., Lomas, M., Piao, S. L., Betts, R., Ciais, P., Cox, P.,
698 Friedlingstein, P., Jones, C. D., Prentice, I. C., and Woodward, F. I.: Evaluation of the terrestrial carbon cycle,



- 699 future plant geography and climate-carbon cycle feedbacks using five Dynamic Global Vegetation Models
700 (DGVMs), *Global Change Biol.*, 14, 2015-2039, <https://doi.org/10.1111/j.1365-2486.2008.01626.x>, 2008.
- 701 Snell, R. S., Huth, A., Nabel, J. E. M. S., Bocedi, G., Travis, J. M. J., Gravel, D., Bugmann, H., Gutiérrez, A. G.,
702 Hickler, T., Higgins, S. I., Reineking, B., Scherstjanoi, M., Zurbriggen, N., and Lischke, H.: Using dynamic
703 vegetation models to simulate plant range shifts, *Ecography*, 37, 1184-1197, <https://doi.org/10.1111/ecog.00580>,
704 2014.
- 705 Song, X., Zeng, X., and Zhu, J.: Evaluating the tree population density and its impacts in CLM-DGVM, *Advances*
706 *in Atmospheric Sciences*, 30, 116-124, <https://doi.org/10.1007/s00376-012-1271-0>, 2013.
- 707 Strand, G.-H.: The Norwegian area frame survey of land cover and outfield land resources, *Norsk Geografisk*
708 *Tidsskrift*, 67, 24-35, <https://doi.org/10.1080/00291951.2012.760001>, 2013.
- 709 Ullerud, H. A., Bryn, A., and Klanderud, K.: Distribution modelling of vegetation types in the boreal–alpine
710 ecotone, *Applied Vegetation Science*, 19, 528-540, <https://doi.org/10.1111/avsc.12236>, 2016.
- 711 Ullerud, H. A., Bryn, A., and Skånes, H.: Bridging theory and implementation – Testing an abstract classification
712 system for practical mapping by field survey and 3D aerial photographic interpretation, *Norsk Geografisk*
713 *Tidsskrift*, 73, 301-317, <https://doi.org/10.1080/00291951.2020.1717595>, 2020.
- 714 Vowles, T., Gunnarsson, B., Molau, U., Hickler, T., Klemedtsson, L., and Björk, R. G.: Expansion of deciduous
715 tall shrubs but not evergreen dwarf shrubs inhibited by reindeer in Scandes mountain range, *J. Ecol.*, 105, 1547-
716 1561, <https://doi.org/10.1111/1365-2745.12753>, 2017.
- 717 Wielgolaski, F. E.: History and Environment of the Nordic Mountain Birch, in: *Plant Ecology, Herbivory, and*
718 *Human Impact in Nordic Mountain Birch Forests*, edited by: Caldwell, M. M., Heldmaier, G., Jackson, R. B.,
719 Lange, O. L., Mooney, H. A., Schulze, E. D., Sommer, U., Wielgolaski, F. E., Karlsson, P. S., Neuvonen, S., and
720 Thannheiser, D., *Ecological Studies*, Springer Berlin Heidelberg, Berlin, Heidelberg, 3-18, 2005.
- 721 Wullschleger, S. D., Epstein, H. E., Box, E. O., Euskirchen, E. S., Goswami, S., Iversen, C. M., Kattge, J., Norby,
722 R. J., van Bodegom, P. M., and Xu, X.: Plant functional types in Earth system models: past experiences and future
723 directions for application of dynamic vegetation models in high-latitude ecosystems, *Ann. Bot.*, 114, 1-16,
724 <https://doi.org/10.1093/aob/mcu077>, 2014.
- 725 Xie, Y., Sha, Z., and Yu, M.: Remote sensing imagery in vegetation mapping: a review, *Journal of Plant Ecology*,
726 1, 9-23, <https://doi.org/10.1093/jpe/rtm005>, 2008.
- 727 Zeng, X., Zeng, X., and Barlage, M.: Growing temperate shrubs over arid and semiarid regions in the Community
728 Land Model–Dynamic Global Vegetation Model, *Global Biogeochemical Cycles*, 22, n/a-n/a,
729 <https://doi.org/10.1029/2007gb003014>, 2008.
- 730 Zhang, W., Brandt, M., Tong, X., Tian, Q., and Fensholt, R.: Impacts of the seasonal distribution of rainfall on
731 vegetation productivity across the Sahel, *Biogeosciences*, 15, 319-330, <https://doi.org/10.5194/bg-15-319-2018>,
732 2018.
- 733 Zhu, J., Zeng, X., Zhang, M., Dai, Y., Ji, D., Li, F., Zhang, Q., Zhang, H., and Song, X.: Evaluation of the New
734 Dynamic Global Vegetation Model in CAS-ESM, *Advances in Atmospheric Sciences*, 35, 659-670,
735 <https://doi.org/10.1007/s00376-017-7154-7>, 2018.
- 736 Zuur, A. F., Ieno, E. N., and Smith, G. M.: *Analysing ecological data*, in, Springer, New York, 163-178, 2007.
737